

Preliminary First Principle Based Electro-thermal Coupled Solver for Silicon Carbide Power Devices

Angie Fan, Greg Troszak, Tapan Desai
Advanced Cooling Technologies, Inc.
1046 New Holland Ave, Lancaster PA 17601
Angie.fan@1-act.com

Tomas Palacios
Massachusetts Institute of Technology
77 Massachusetts Avenue Cambridge, MA 02139

Massoud Kaviani, Seungha Shin
University of Michigan
4260 Plymouth Road, Ann Arbor, Michigan, 48109

Abstract

The electrical behavior of high power, high frequency power devices is dramatically affected by heat generation caused due to interactions between energetic electrons and the lattice. It is critical that these interactions are taken into account when attempting to predict the electrical behavior of these devices. Since the hydrodynamic model follows the mass, momentum and energy transfer between the electrons/holes and phonons, it is capable of simultaneously predicting the electrical and thermal performance of these devices. This model is accurate and computationally efficient when properly correlated material parameters are available. In this work, a preliminary hydrodynamic transport device solver capable of accurately predicting the thermal and electrical performance of SiC devices is presented.

Keywords

SiC power switching devices, transient temperature solver, hydrodynamic approach

Nomenclature

C_A	Acoustic phonon heat capacity, J/kg-K
C_{LO}	Optical phonon heat capacity, J/kg-K
E	Electric field, V/m
e	Elementary (electron) charge, $1.60217653 \times 10^{-19}$ C
k_A	Acoustic phonon thermal conductivity, W/m-K
k_B	Boltzmann constant, 1.381×10^{-23} J/K
k_e	Electron thermal conductivity, W/m-K
m^*	Electron effective mass, kg
n or n_d	Electron concentration rate, m^{-3}
N_A	Doping rate of holes, m^{-3}
N_D	Doping rate of electrons, m^{-3}
p	Hole concentration rate, m^{-3}
t	Time, s
T_A	Acoustic phonon temperature, K
T_e	Electron temperature, K
T_{LO}	LO-phonon temperature, K

Greek

$\dot{\gamma}$	Phonon emission rates, 1/s
ϵ	Permittivity, F/m
μ_h	Electron mobility, $m^2/V\cdot s$
μ_p	Hole mobility, $m^2/V\cdot s$
v_D	Electron drift velocity, m/s
τ_{e-LO}	Electron - optical phonon energy relaxation time, s
τ_{LO-A}	Optical - acoustic phonon energy relaxation time, s
τ_m	Electron momentum relaxation time, s

1. Introduction

In recent years, silicon carbide (SiC) devices are reaching a level of performance that affords significant advantages in high power switching applications relative to silicon due to their high breakdown voltage, low on-resistance and high thermal conductivity [1-8]. To address the reliability issues associated with high device temperatures, the self-heating effects in SiC-based high power switching devices needs to be characterized. The heat generation rate in such devices is low to moderate in the off-state and on-state, but intense bursts of power occur during the short switching transitions (20-50 ns). Accurate prediction of the junction temperatures requires a transient thermal model.

The drift-diffusion model is the core in most device simulation packages, which provides robust steady-state simulation in conventional silicon based devices where constant device temperatures are assumed. To update the device temperatures, a simple thermal model based on Fourier's Law is solved separately after the electrical analyses. This method cannot handle the transient heat generation and the instant effects of temperature change on the electrical behavior. A better solution is to couple an equilibrium energy model with the electrical model. This model assumes thermal equilibrium between electrons and phonons. This assumption is proper in most cases except during fast transitions and velocity overshoot. During the non-equilibrium heat generation and transfer, the temperature rise in electrons is much faster and greater than that in phonons, which alters the electrical behavior concurrently. In addition, since most of the mature device solvers were first developed

and fine-tuned for silicon and gallium arsenide, convergence problems arise when new materials such as SiC or GaN are implemented.

Therefore, in this paper we report a preliminary modeling effort using a hydrodynamic approach for improved accuracy in predicting device temperatures in SiC-based power devices. In order to establish a robust transient solver, a steady-state solver was first established. The preliminary results and issues encountered in the modeling are reported in this paper. In future work, the time derivative term will be added to the solver.

2. Model Description

The hydrodynamic approach [9,10] captures the non-equilibrium energy transfer which is ignored by the drift-diffusion approach. The hydrodynamic approach is derived from the first three moments of the Boltzmann Transport Equation (BTE), rather than the first two as in the drift-diffusion approach. The first and second moments of the BTE describe the mass and momentum conservation. The third moment accounts for the energy conservation between electrons and phonons. The Poisson equation, which solves the electro-potential changes in a device, along with the BTEs makes up the hydrodynamic device model. By solving this model, the electric potential, the electron number density (current) and the temperatures of electrons and phonons are updated simultaneously. The model is composed of six equations [11]:

$$\nabla^2 V = -\frac{e}{\epsilon_s} (N_D - n) \quad (1)$$

where $\vec{E} = -\nabla V$

$$\frac{\partial n}{\partial t} - \nabla \cdot (n\mu\vec{E}) - \nabla \cdot \left\{ \frac{\mu}{e} \nabla (nk_B T_e) \right\} = 0 \quad (2)$$

$$\frac{\partial p}{\partial t} - \nabla \cdot (p\mu\vec{E}) + \nabla \cdot \left\{ \frac{\mu}{e} \nabla (pk_B T_e) \right\} = 0 \quad (3)$$

$$\begin{aligned} \frac{\partial T_e}{\partial t} + \nabla \cdot (\vec{v} T_e) &= \frac{1}{3} T_e \nabla \cdot \vec{v} + \frac{2}{3nk_B} \nabla \cdot (k_e \nabla T_e) \\ &+ \frac{m^* v^2}{3k_B} \left(\frac{2}{\tau_m} - \frac{1}{\tau_{e-LO}} \right) - \frac{T_e - T_{LO}}{\tau_{e-LO}} \end{aligned} \quad (4)$$

$$C_{LO} \frac{\partial T_{LO}}{\partial t} = \frac{3}{2} nk_B \frac{T_e - T_{LO}}{\tau_{e-LO}} + \frac{nm^* v^2}{2\tau_{e-LO}} - C_{LO} \frac{T_{LO} - T_A}{\tau_{LO-A}} \quad (5)$$

$$C_A \frac{\partial T_A}{\partial t} = \nabla \cdot (k_A \nabla T_A) + C_{LO} \frac{T_{LO} - T_A}{\tau_{LO-A}} \quad (6)$$

In this study, a two-dimensional steady-state numerical simulation was carried out as follows: first, the equilibrium electrostatic potential of the device was solved from the Poisson equation (Eq.1). Then the Poisson (Eq.1) and the continuity equations (Eq.2 and Eq.3) for both electron and hole number densities were solved. Once convergence was reached, the results were passed on to the energy conservation equations Eq.4-Eq.6. The outcome temperatures were fed back to the electrical solver (Eq.2 –Eq.4) until convergence was reached. A control volume method was used to discretize

the equations. Gummel's method [12] was used to decouple the nonlinear equation system. The Scharfetter-Gummel algorithm [13] was used for solving the momentum and energy equations. The mesh size was chosen to be smaller than the Debye length to reduce the error due to discretization [14].

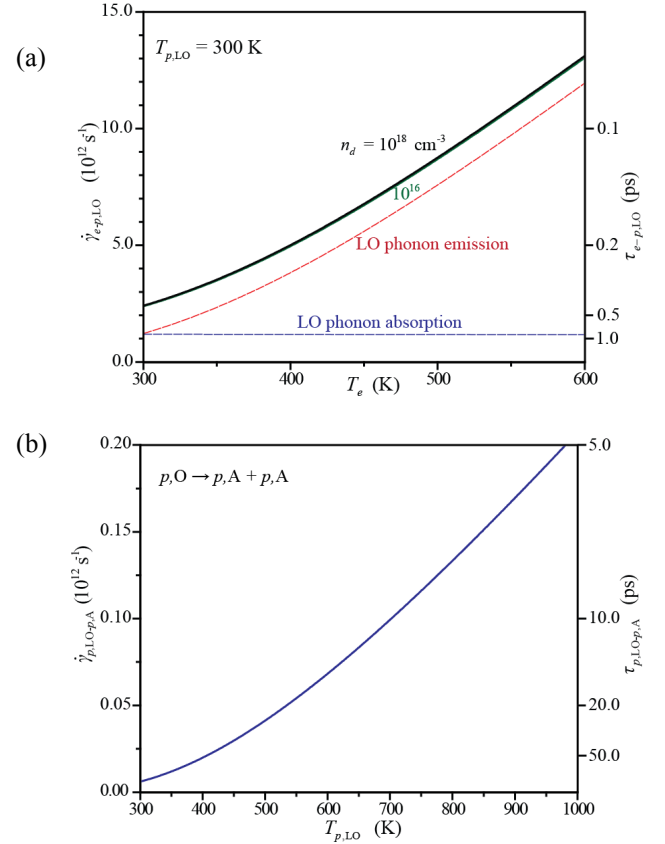


Figure 1: Energy relaxation times τ (1 / phonon emission rates $\dot{\gamma}$) for 4H-SiC. (a) Electron-LO phonon energy relaxation time is a function of electron temperatures and doping rates. (b) LO-acoustic phonon energy relaxation time is a function of LO-phonon temperature.

Material properties are also critical for accurate simulation. In this study, we performed intensive literature study and calculation for the following temperature dependent properties for 4H-SiC: electron mobility, hole mobility, energy relaxation times, electron thermal conductivity, acoustic phonon thermal conductivity, LO-phonon specific heat, and acoustic phonon specific heat. Among these properties, the energy relaxation times and electron mobility (or drift velocity) are crucial. This can be explained by understanding the energy transfer process.

The electrons obtain the energy from the electric field instantly. Once energized, the electrons start to move from the source to the drain, colliding with the lattice along the path, and convert the energy to the lattice. When the electrons' energies are high enough, they emit the longitudinal optical (LO) phonons. Figure 1(a) shows that the energy relaxation time between the electrons and LO-phonons is less than 1 ps. Further scattering with the LO-phonons, the drift velocity of the electrons is saturated or reduced as shown in Figure 2. Since the LO-phonons are static, they need to become

acoustic phonons to transfer the heat to the ambient. The relaxation time between the LO-phonons and acoustic phonons are about 5~50 ps as Figure 1(b) indicated. It takes another 1 ms – 1 s for the acoustic phonons to travel to the boundary of the package. Therefore, if the transitions are short enough, non-equilibrium energy transfer can occur. Electrons can be much hotter than the phonons. Since the electron mobility is related with the electron temperature, ignore the electron temperature can lead to false prediction in electrical outputs.

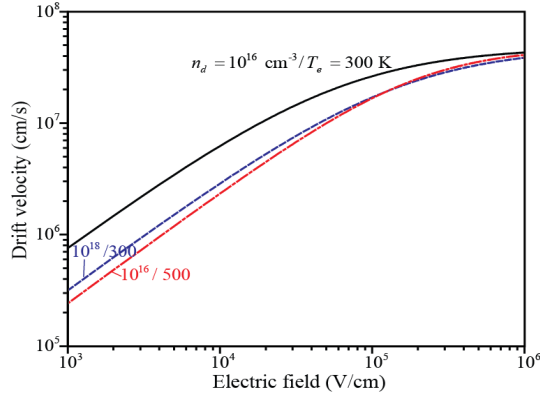


Figure 2: Drift velocity in 4H-SiC is a function of electric field, electron number density n_d and electron temperature T_e . In the low field region, the drift velocity is proportional to the electric field. In the high field, the drift saturates and becomes independent of the electron number density and electron temperature.

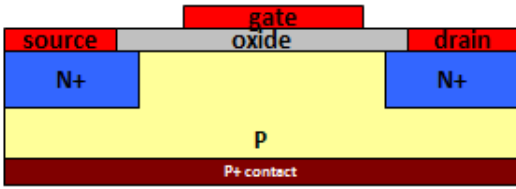


Figure 3: A simple SiC MOSFET device for validation ($1\mu\text{m} \times 0.6\mu\text{m}$)

Figure 3 shows a cross sectional view of a simple MOSFET device for validation. This is a normal-off MOSFET. When no gate voltage is applied (off-state), current flow between the source and drain is blocked. When a gate voltage is applied (on-state), an inversion layer of electrons appears in the p-doped region under the gate and forms the channel. Electrons flow into the device via the source contact, through the channel underneath the oxide layer, and then flow out from the drain contact.

3. Preliminary Results

Due to the complexity of the model, the validation of the device solver was divided into two steps. In the first step, only the electrical part was solved. Once validated, the thermal part was then coupled. The results are presented in the following part.

3.1. Electrical Solver

The electrical solver assumed that the device temperature was uniform and constant. Figure 4 and Figure 5 show the

calculated results from the electrical solver. The calculated electrostatic potential in Figure 4(a) is for a drain to source voltage of 2.6 V and a gate to source voltage of -1 V. Responding to the applied bias, the electrons redistributed in the device (Figure 4(b)). No electron channel is formed under this condition. This is the OFF-state. In Figure 5(a), the drain to source voltage is 0.1 V and the gate to source voltage is 5V. The applied bias expelled the holes under the gate and an electron channel is formed in Figure 5(b).

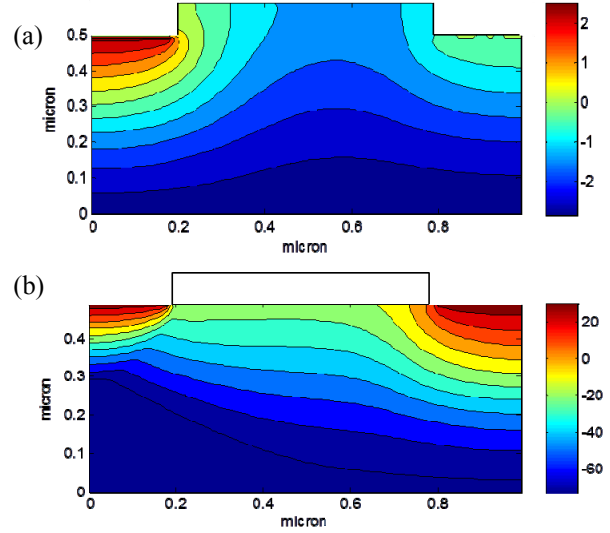


Figure 4: OFF-state ($V_{ds} = 2.6\text{V}$, $V_{gs} = -1\text{V}$). (a) Potential V, Volts; (b) electron number density n , cm^{-3} in log scale

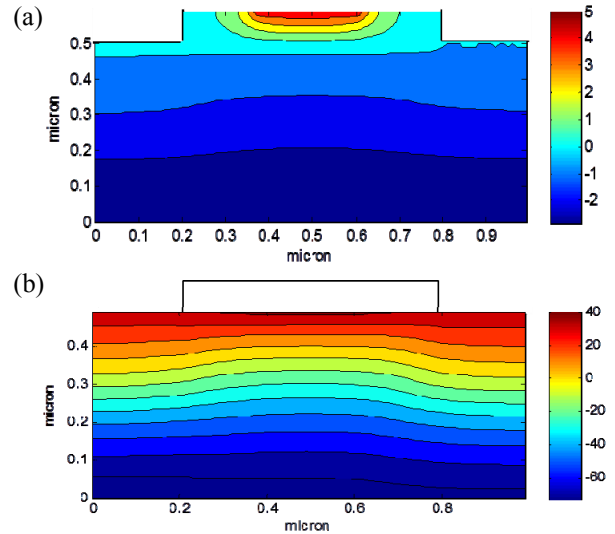


Figure 5: ON-state ($V_{ds} = 0.1\text{V}$, $V_{gs} = 5\text{V}$). (a) Potential V, Volts; (b) electron number density n , cm^{-3} in log scale

The calculated I-V curves for the MOSFET device under different gate voltages (1 V, 5 V, 10 V, and 15 V) is shown in Figure 6 and compared with experiments from [7]. The trend of drain currents varying in response to the applied bias agrees with experiments. The size of the reference device was larger than ours. In practice, drain currents are inversely proportional to the device sizes. Under $V_{gs} = 10\text{V}$ and $V_{ds} = 3\text{V}$, the drain current was 1 A/m from our device, and it was 0.1 A/m from

the reference device. Therefore, the preliminary results from our solver were reasonable both in magnitude and behavior. More validations with experiments are needed.

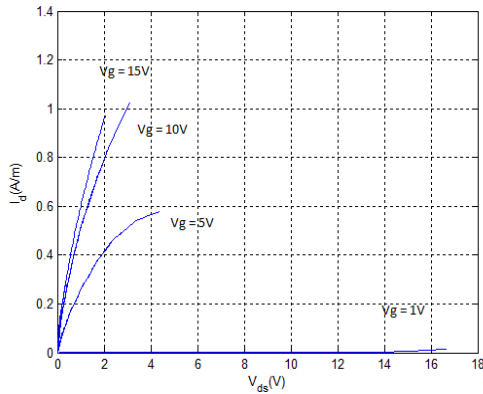


Figure 6: Calculated I-V curve under varying gate bias (1V, 5V, 10V, 15V)

At elevated bias, our solver slowed down and had difficulty in converging. This is because the coupling between equations gets stronger as the bias increases. Gummel's method is less robust at high bias. Instead, at high bias, Newton's method needs to be used after the initial iterations to improve the computational efficiency. This hybrid method will be implemented in future work.

3.2. Preliminary Electrical and Thermal Coupled solver

In reality, the device temperature is neither uniform nor constant. By coupling a set of energy conservation equations (Eq.4 – Eq.6) to the electrical solver, more accurate device temperatures and the electrical behavior can be predicted. The preliminary results for the electro-thermal coupled solver are shown in

Figure 7. The applied gate to source voltage is 10 V, and the drain to source voltage is 2.2 V.

Figure 7(a) shows the electric field of the device, where high electric field occurs under the gate.

Figure 7(b) shows the electron number density. The highest electron density appears under the oxide layer and SiC interface; this is the location of the electron channel.

Figure 7(c) shows the electron current density. High current density only appears in the channel while the rest of the device has no current.

Figure 7(d) shows the electron temperature. The maximum electron temperature increases significantly from 300 K to 3000 K in the channel toward the drain side. The location of the hot spot and the magnitude of the maximum electron temperature agreed with the results from [15,16], where similar sizes GaAs and GaN MESFETs were simulated. However, at high bias, numerical error is introduced into the channel as the hole number density becomes very close to zero. This error affected the electron temperature solver, as can be seen in the channel in

Figure 7(d). The error quickly propagated and inhibited the iterations between the energy solvers. Remedy for this error by applying numerical filters is under investigation.

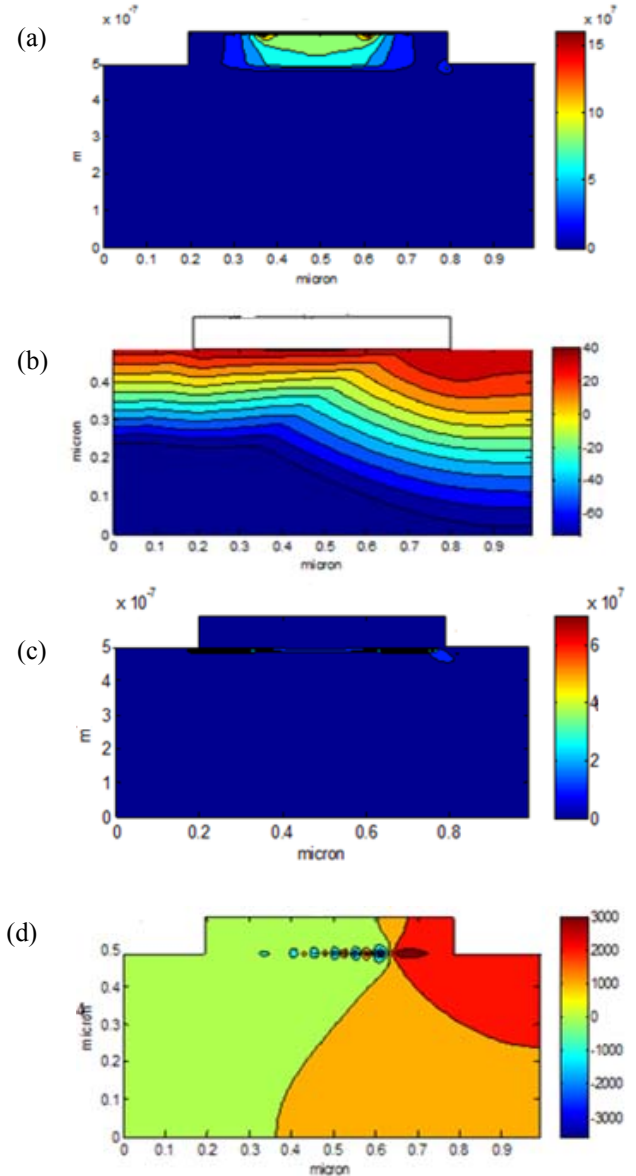


Figure 7: Calculated result under $V_{ds} = 2.2$ V and $V_{gs} = 10$ V. (a) Electric field E , V/m; (b) electron number density n , cm^{-3} in log scale; (c) electron current density J , A/m²; (d) electron temperature T_e , K.

4. Conclusions

SiC-based devices have superior performance in high-voltage power switching applications due to their high breakdown voltage, low on-resistance and high thermal conductivity. However severe self-heating occurs during the short switching transitions (20-50 ns). Therefore, accurate transient modeling of the device temperature is critical to address the device reliability.

The paper presents the preliminary effort toward developing a transient device solver using the hydrodynamic approach. In this approach, the electrical and thermal models (six non-linear PDEs) are solved concurrently to capture the interactions between the electrical outputs and the device

temperatures. To reduce the complexity of the problem, validation of the solver was performed step by step. First, the steady-state electrical model was established and validated. Then the electrical model was coupled with a steady-state thermal model to build a complete steady-state device solver. Later, time derivative terms will be added back to the steady-state solver to make it transient. Once validated, the solver will be fine-tuned to adapt different device structures and various types of SiCs. The preliminary results and issues for the first two steps are discussed in this paper. Reasonable electrical behaviors and outputs were generated from the steady-state electrical solver. When coupled with the electron energy solver, proper location and magnitude of the electron temperature was obtained. More work and validation are needed to fix the convergence issue and numerical error occurred under high applied bias.

Acknowledgments

This material is based upon work supported by the U.S. Army, RDECOM Contracting Center, and Under Contract No. W911QX-12-C-0046.

References

1. Cooper, J. A., Tamaki, T., Walden, G. G., Sui, Y., Wang S. R., Wang, X., "Power MOSFETs, IGBTs, and Thyristors in SiC: Optimization, Experimental Results, and Theoretical Performance", Electron Devices Meeting (IEDM), 2009 IEEE International, pp. 1-4, 2009
2. Singh, S., Cooper, J. A., "Bipolar Integrated Circuits in 4H-SiC", IEEE Trans on electron devices, Vol. 58, No. 4, pp. 1084 – 1090, 2011
3. Loh, W. S., Ng, B. K., Ng, J. S., Soloviev, S. I., Ho-Young Cha, Sandvik, P. M., Johnson, C. M., David, J. P. R., "Impact Ionization Coefficients in 4H-SiC", IEEE Trans on electron devices, Vol. 55, No. 8, pp. 1984 – 1990, 2008
4. Cooper, J. A., Agarwal, A., "SiC Power-Switching Devices – the Second Electronics Revolution?", Proceedings of the IEEE, Vol. 90, No. 6, pp. 956 – 968, 2002
5. Kimoto, T., Kawano, H., Suda, J., "1330 V, 67 mΩ·cm² 4H-SiC(001) Resurf MOSFET", IEEE Electron Device Letters, Vol. 26, No. 9, 2005
6. Sei-Hyung Ryu, Krishnaswami, S., Das, M., Richmond, J., Agarwal, A., Palmour, J., "2 KV 4H-SiC DMOSFETs for Low Loss, High Frequency Switching Applications", Proc of IEEE Lester Eastman Conference on High Performance Devices, pp. 255-259, 2004.
7. Saha, A., Cooper, J. A., "A 1-kV 4H-SiC Power DMOSFET Optimized for Low ON-Resistance", IEEE Transactions On Electron Devices, Vol. 54, No. 10, pp. 2786-2791, 2007
8. Yutian Cui, Chinthavali, M. S., Fan Xu, Tolbert, L. M., "Characterization and Modeling of Silicon Carbide Power Devices and Paralleling Operation", 2012 IEEE International Symposium on Industrial Electronics(ISIE), pp. 228-233, 2012
9. Blotekjaer, K., "Transport Equations for Electrons in Two-valley Semiconductors", IEEE Trans. on Electron Devices., Vol. 17, No. 1, pp. 38-47,1970
10. Chang-Lin Tien, Majumdar, A., Gerner, F., M., Microscale Energy Transport, Taylor & Francis, 1998, pp. 88
11. M. Kaviany, Heat Transfer Physics, Cambridge University Press, 2008
12. Gummel, H. K., "A self-consistent iterative scheme for one-dimensional steady state transistor calculations", IEEE Transactions on Electron Devices, Vol. 11, No. 10, pp. 455-465, 1964
13. Forghieri, A., Guerrieri, R., Ciampolini, P., Gundi, A., Rudan, M., Baccarani, G., "A New Discretization Strategy of the Semiconductor Equations Comprising Momentum and Energy Balance", IEEE Trans. Computer-aided Design CAD, Vol. 7, No. 2, pp. 231-242, 1988
14. Sze, S. M., Physics of Semiconductor Devices, 2nd ed., Wiley, New York, 1986
15. Majumdar, A., Fushinobu, K., Hijikata, K., "Effect of Gate Voltage on Hot-electron and Hot-phonon interaction and transport in a Submicrometer Transistor", J. Appl. Phys., Vol. 77, No. 12, pp. 6686, 1995
16. Fan, A., Tarau, C., Bonner, R., Palacios, T., Kaviany, M., "2-D Simulation of Hot Electron-phonon Interactions in a Submicron Gallium Nitride Device using Hydrodynamic Transport Approach", ASME 2012 Summer Heat Transfer Conference, 2012